Design of a Novel Hybrid Rice Straw/Husk Bio-Based Concrete Featuring The Enhanced Mechanical and Hygrothermal Properties

Youssef El Moussi, Laurent Clerc, Jean-Charles Benezet

Design of a Novel Hybrid Rice Straw/Husk Bio-Based Concrete Featuring The Enhanced Mechanical and Hygrothermal Properties

Youssef EL MOUSSI
IMT Mines Alès: Institut Mines-Telecom Mines Ales https://orcid.org/0000-0002-1373-384X
Laurent CLERC (laurent.clerc@mines-ales.fr)
IMT Mines Alès: Institut Mines-Telecom Mines Ales
Jean-Charles BENEZET
IMT Mines Alès: Institut Mines-Telecom Mines Ales

Research Article

Keywords: bio-based materials, Rice straw, Rice husk, Thermal conductivity, Mechanical behavior, Moisture buffering potential.

Posted Date: February 24th, 2022

DOI: https://doi.org/10.21203/rs.3.rs-1315395/v1

Abstract

In order to reduce the consumption of energy and the emissions of greenhouse gases and CO_2 generated by the construction industry, bio-based concretes made of plant aggregates are increasingly used in the optimization of building envelopes thanks to their good hydrothermal performances, their renewable origin, and biodegradability. These insulation materials are considered as a promising alternative to synthetic systems made of mineral wool.

This study investigates the use of a bio-based concretes performed with a mixture of eco-aggregates derived from rice plant and lime as thermal insulation materials. The effect of combining different proportions of rice straw (RS) with rice husks (RH) (100%, 66%, 50%, and 33%) on both mechanical and hydrothermal properties of bio-based concretes are investigated. The characterization seeks to evaluate the thermal conductivity, moisture buffer value (MBV) and mechanical compressive properties of the rice straw/rice husk concretes. Results show that the thermal conductivity of the bio-based concretes slightly decreased with increasing rice straw content. The MBV values measured showed that rice straw confers to concretes an excellent moisture buffering capacity according to the Nordtest project classification. The compression test result also revealed that rice straw concretes have high mechanical deformability. Straw concretes do not break but continuously deform.

Statement Of Novelty

The novelty of this manuscript lies in mixing rice straws and rice husk particles in order to design a hybrid lightweight insulation material. In general, rice husk and rice straw are used separately with various matrices, but the combination of rice husk and rice straw using lime as a matrix has not been yet explored. This manuscript evidences clearly that it is interesting to associate these two residues, in fact the negativity of one aggregate is neutralized and compensated by the positivity of another aggregates. The results showed that the hybrid concretes perform better compared to the pure rice husk concretes. Indeed, the addition of straw leads to lighter concrete and helps to lower the thermal conductivity of concretes.

1. Introduction

Building sector is the largest energy consumer in Europe and the US accounting for more than 40% of the total energy consumption and responsible for emitting one-third (36%) of associated greenhouse gases, particularly because of heating, cooling, and air conditioning systems according to the European Commission [1, 2]. Within this context, and in order to achieve significant energy savings and reduce CO_2 emissions, the European Commission has established a set of binding directives [3]. Which aim to achieve at least 32.5% energy efficiency for 2030 and give birth to the concept of nearly zero-energy buildings (NZEBs), this latter, require a minimum amount of energy for operations (i.e. for heating, cooling, lighting, and other appliances), mainly coming from renewable sources [4].

Enhancing the thermal insulation properties in building envelopes represents a key step in minimizing the energy demand for winter heating and summer cooling purposes of buildings [5]. Up to now, building envelopes are mainly realized with traditional insulation materials obtained from fossil energy such as expanded polystyrene or from mineral origin such as glass and rock wools. However, in the context of sustainability and environmental protection, alternative materials such as bio-aggregate-based concretes are developed by combining plant origin aggregates which are renewable and local resources with mineral binders, in order to replace conventional thermal insulation materials and reduce non-renewable resources consumption [6, 7]. Indeed, researches, showed that bio-based concretes are highly suitable for building applications since they exhibit an excellent thermal performance and enable moisture management by adsorbing and desorbing water vapor[8–10]. Moreover, they allow to design a carbon negative building material due to carbon sequestration, thanks to the absorption of CO_2 present in the atmosphere through photosynthesis during the plant's growing stage, and to the absorption of high quantities of CO_2 during the carbonation of lime (curing process) [11–12]. In fact, according to Boutin et al. [13] and Ip and Miller [14], hemp concretes enables to store approximately 0.35-0.36 kg of CO_2 eq per square meter of wall built (with a thickness of 25-30 cm) over a year.

In this sense, several researches researchers have explored the possibilities of the incorporation of other lignocellulosic aggregates in concretes to develop an alternative/similar concrete to lime hemp concrete. Indeed, bio-based concretes are currently manufactured from different vegetable aggregates, such as hemp hurds [15–17], sawdust of sunflower [18–19], flax shives[20], and rice husk [21–23]. Some advantages of these particles include their very low density, very low thermal conductivity, and high hygroscopic property. Additionally, they have a short growing period and annual harvest.

Thus far, the widely studied bio-based lightweight concretes are concretes, however, in the previous study conducted by Chabannes et al.[23], rice husk concrete was found to have a very low thermal conductivity (0.10–0.13 W. $m^{-1}.K^{-1}$) depending on aggregates to binder ratio, these values of the thermal conductivity coefficient are comparable to those of hemp concrete (0.09–0.13 W .m^{-1}. K^{-1}). Add to that, Nozahic et al. [24], find that hemp and sunflower concretes show large similarities in terms of mechanical performance. In another study, Rahim et al.[25] compared hygric properties of lime concrete made of rape straw with hemp lime concrete, the results show that the MBV values for both concretes are higher than > 2.0 g/(m^2 .%RH), therefore, both concretes exhibit an excellent moisture buffer capacity.

In the case of straw based building materials, Belayachi et al. [26] investigated the use of wheat and barley straw in lime concretes for thermal insulation applications and studied the influence of the type of straw and straw to binder ratio (S/B) on the mechanical and thermal properties. The results indicated that concretes prepared with wheat straw have the highest compressive strength, while, the thermal conductivity of concretes decreased with increasing straw content. Moreover, Labat et al.[27], investigated the hygrothermal properties of straw-clay concretes and compared them to bio-based materials, results revealed that straw-clay concretes showed a high sorption capacity, a very high water vapor permeability

and a low thermal conductivity (ranging from 0.071 to 0.120 W .m^{-1}.K^{-1}) which is comparable with hemp concretes conductivity of equivalent density.

Furthermore, Belhadj et al. [28, 29], used barley straws fibers (0.08, 0.16 and 0.24 wt%) in order to lightweight sand concretes. While, Xin Chen et al [30], utilized rice straw to prepare cemented tailings backfill, and studied the effect of the rice straw content and length on compressive strength and elastic modulus. Results highlight the improvement of the stiffness and ductility of the rice straw cemented tailings backfill with increasing fiber content and length.

However, there is a remarkable lack of research on the use of rice straw in bio-based concretes. For instance, rice straw is often burned in the field to remove rice residues left in the field after harvesting grains. Or burnt to produce ashes which could be used in lime and cement-based system due to its high amount of silica which might improve its mechanical properties [31]. Nonetheless, this practice has negative impacts on the environment, in fact, rice straw open field burning leads to air pollution and contributes to global warming through emissions of greenhouse gases [32–34].

To sum up, based on the findings reported on mechanical and hygrothermal properties of straw concretes, and on the negative impacts of burning straw on the environment, their use of rice straw in insulation materials could be highly recommended in buildings for its ability to lower heat transfer and to moderate indoor humidity variations. Also, the use of rice straw in the preparation of concretes can be considered as an environmental protection measure.

To the best of our knowledge, the combination of rice straw with other plant aggregates in bio-based concretes has not yet been investigated. Otherwise, a recent study conducted by Page et al[35], on a hybrid hemp-flax concrete showed that the incorporation of the flax fibers increased the ductility and improved the compressive strength of hemp concrete. It seems interesting to associate the two residues of rice production. Hence, the present work explores the influence of the mixture rice straw to rice husk ratio (RS/RH) at different ratios on the mechanical and hygrothermal characteristics of hardened bio-based concretes. The lightweight concretes were performed with different mixes of rice straw-rice husks at the same binder/aggregates ratio and different densities (fresh density less than 1000 kg/m^3). Indeed, the effect of combining different proportions of rice straw (S) with rice husks (H) (100%, 66%, 50% and 33%) on both mechanical and hygrothermal proprieties of five bio-based concretes were highlighted so as to identify the best straw-husks mixture.

2. Materials And Methods

2.1. Materials

2.1.1. Mineral Binder

Concretes were prepared with a binder composed of a 50/50 wt% combination of aerial calcic lime (CL90-S) and natural hydraulic lime (NHL 3.5). Hydraulic lime NHL3.5 and aerial calcic lime CL90-S were provided from (Saint-Astier, France). According to Chabannes et al.[22], the amount of $Ca(OH)_2$, C_2S and $CaCO_3$ in the mixture of NHL3.5 and CL90-S at 50/50 wt.% were 65 wt.%,15 wt.% and 10 wt.%, respectively.

2.1.2. Plant Aggregates

The untreated rice husk and whole rice straw were collected from Aigues-Mortes in the Camargue province of France (late cultivated season). Their biochemical composition was characterized according to the ASTM method (standards NF EN ISO). The dried rice straw was carefully cut into particles of 4 and 6 cm lengths by manual cutter (scissors). It was not longitudinally cut to ensure the cylindrical shape and save its intra-granular porosity. It should be noticed that only the rice straw obtained from the upper part of the stems plant and consisting of stem and leaf blade were used in this study. The designations of the rice husk and rice straw are respectively: RH and RS.

2.2. Preparation and manufacturing of concretes

Two eco-aggregates derived from rice plant were used to manufacture the composite specimens and five different mixtures corresponding to different rice husk-rice straw mass ratios different proportions of rice straw (RS) with rice husks (RH) (100%, 66%, 50%, and 33%) were prepared and investigated in order to determine the optimal composite.

All mixtures were performed with a binder-to-aggregate mass ratio (B/A) of 2, the mixing water-to-binder mass ratio (W_m/B) was taken as 0.5, and the pre-wetting water (W_p) was calculated from the water test capacity of aggregates after 5 min. The mixing process was identical for each formulation; the procedure consisted in:

-Pre-wetting of natural particles for 5 minutes before incorporating the binder.

-In second, the binder was added and combined with the particles for 2 minutes

-At last, water was added and mixed for five minutes until complete homogeneity was obtained.

The fabrication of concrete has been performed manually by a molding method in 3 layers of the same weight and same height. Concrete specimens were manufactured using manual compaction in 11x22 cm^3 cylindrical molds with a steel device [23, 24]. Special attention has been taken to achieve a similar compaction force for all concretes. The upper surface is kept smooth and a cover is put on the top of specimens. As each aggregate has a different density and water content, which depends on its composition and structure, the fresh apparent density of concretes could not be kept constant. Therefore, it was based on workability which was consistent in all concretes. Specimens were demolded after three days and stored in a conditioned room at 20°C and 50%HR until testing in order to ensure complete and

rapid carbonation of concrete[36]. The mix proportions and the fresh density of all samples are reported in Tab. 1.

Table 1
designation and corresponding formulation of concretes

Mixture	W/B	Binder (kg/m^3)	Aggregates (kg/m^3)	W_p (kg/m^3)	W_m (kg/m^3)	Fresh density (kg/m^3)
100%RH	0.88	410	205	158	205	980
33% RS	1.07	380	190	219	190	980
50% RS	1.17	366	183	246	183	900
66% RS	1.26	288	144	222	144	800
100%RS	1.46	270	135	259	135	800
W/B is the water-to-binder mass ratio.						

2.3. Characterization of natural particles

2.3.1. Chemical composition analysis of plant particles

Composition analyses were performed using a successive solvent extraction procedure according to the following ASTM standards: alpha-cellulose (ASTM D1103-60), lipophilic extractives (ASTM D1107-56) and holocellulose (ASTM D 1104-56) used in previous studies[37–39]. It can be divided into three steps:

1st step: determination of lipophilic extractives (waxes, fats, resins and some gums) using Soxhlet extractor. A mixture of toluene/ethanol (2:1 w/w) was used as solvent and the extraction process continued for 8 h.

2nd step: holocellulose extraction was carried out using a fraction of the previously extracted sample. Water, acetic acid and sodium chlorite ($NaClO_2$) was used for the extraction process. lignin ratio was calculated from holocellulose residue.

3rd step: α-cellulose was finally obtained by hemicelluloses solubilization in sodium hydroxide solution (NaOH) and acetic acid. Finally, inorganic components were determined according to (ASTM D 1102-84) method. where dried particles were ignited in the oven at 600°C for 8 h. and the heating was repeated until all the carbon is eliminated. It should be noticed out that, the resulting holocellulose, α-cellulose, and ashes were weighed using the IR balance (Precisa XM66) at 105°C.

2.3.2. Morphological investigations

Plant aggregate microstructure morphology was carried out by means of the environmental scanning electron microscope (ESEM FEI Quanta 200) equipped with a XMAX 80 mm² Oxford Instrument detector

used to determine the silica location on the particles. A layer of carbon was deposed on the surface of particles in order to avoid any degradation during analysis. Samples were examined under high vacuum with an accelerating voltage of 10 kV and a working distance between 10 and 20 mm.

3.3.3. Particles size distribution

Granulometric analysis of plant aggregates was performed using an image analysis processing according to RILEM TC 236-BBM [40] group recommendations using ImageJ software. The same approach was used by several authors [15, 41], which is suitable for determining the lignocellulosic particle aggregate. It yields to accurate information such as the minor and the major axis (width and length), and the equivalent area diameter that can be calculated according to Eq. (1).

$$\varphi = \sqrt{\frac{4Area}{\pi}}$$

1

It consists of spreading particles on a black paper. Then, particles are scanned with a numerical camera with high pixels' resolution (digital acquisition). Several image treatments are performed to correct the picture, involving the creation of binary images of the particles from color images and correcting of brightness/contrast, and then software analysis particle dimensional and morphological characteristics were realized. The particle shape is defined by its aspect ratio (L/W), i.e. the ratio between length (L) and width (W).

3.3.4. Water sensitivity of particles

The water absorption ability of plant aggregates was measured according to the recommendation of the RILEM TC 236-BBM [40], by placing dried particles (48 h at 105°C) in a metallic permeable bag and immersion of the bag in water until a complete wetting. This was repeated at different immersion times (after 1, 2, 5, 10, 30 minutes and 48 h). Then, particles were centrifuged using a spinner in order to extract the water excess present between the particles and on particles' surface due to their open capillary pore structure and sensitivity to water. The water uptake was measured at given time intervals up to a maximum of 48 h. The absorption coefficient WA (water absorption ratio) was estimated and used to determine the amount of pre-wetting water mass. Tests were repeated 3 times (with 3 different samples of particles). The water absorption coefficient (WA) of aggregates was calculated using the Eq. (2).

$$WA(t) = \frac{(m(t) - mi)}{m(t)} \times 100$$

2

Where WA (t) is the water absorption ratio at time t, m(t) [g] is the soaked aggregate mass at time t, and mi[g] is the initial mass of dry aggregates.

3.3.5. Density measurements and porosity estimation.

3.3.5.1. Density measurements

Bulk density of natural particles is measured using protocols set by RILEM TC 236-BBM [40], by filling a cylindrical mold of 11 cm in diameter and 22 cm in height with particles without compaction (using the standard mass over volume formula). Prior to measurements, particles were dried at 100°C until the constant mass is reached and then cooled in a desiccator until room temperature (23°C, 50%RH). Measurements are repeated five times.

The absolute density excluding pores was measured with a helium pycnometer (AccuPyc 1330, Micromeritics, Norcross, GA, USA).

The Apparent particle density was calculated from the absolute density and the water absorption capacity of particles after saturation (W_{max}) according to Eq. (3).

$$\rho_a = \left(1 - \eta_0\right).\rho_t$$

3

whereρ_t is the particles absolute density and $\eta_0$is the open porosity in the particle obtained with the expression Eq. (4).

$$\eta_0 = \frac{W_{max}.\rho_t}{\rho_w + (W_{max}.\rho_t)}$$

4

where ρ_t is the known absolute density, $\rho_w$is the density of water and W_{max} is the water absorption capacity of particles after saturation **(48h)**, W_{max} was taken as 110% for rice husk and 350% for rice straw based on water absorption capacity measurements.

Furthermore, the apparent density of concretes was measured based on the weight and the volume of the samples, three replicate samples were used for the test.

3.3.5.2. Porosity estimation of concretes

Knowing the densities of a different constituent, as well as their weight, the volumes occupied by each constituent were calculated and thus volume occupied by void is concluded. According to Chabannes et al .[42], the inter-particles and total porosities into the bio-based concretes can be calculated according to the Eq. (5) and Eq. (6).

The total porosity (including micro-porosity of the binder and capillary voids within rice plant particles) was deduced using the absolute density of lime and straw particles knowing the volume occupied by each component in the mold.

$$\eta_{total}(\%) = \frac{Vpores}{Vs} = \frac{V_s - (\frac{M_{lime}}{\rho_{abs-l}} + \frac{M_{RH}}{\rho_{t-RH}} + \frac{M_{RS}}{\rho_{t-rs}})}{V_s} \times 100$$

5

On the other hand, inter-granular porosity can be deduced with the total volume of the specimen which is known using this time the apparent density of binder paste and the apparent density of a single particle.

$$\eta_{macro}(\%) = \frac{V_s - (\frac{M_{lime}}{\rho_{ap-l}} + \frac{M_{RH}}{\rho_{ap-RH}} + \frac{M_{RS}}{\rho_{ap-rs}})}{V_s} \times 100$$

6

M_{lime}, M_{RH}, M_{RS} is the mass of lime, rice husk and rice straw introduced in the specimen, where ρ_t is the particles absolute density, ρ_{ap} is the apparent density of the constituent ρ_{abs} is the absolute density of the binder and V_S is the volume of the specimen. The apparent density of the binder paste was taken as 840.3 ± 31.8 kg/m^3 according to Chabannes et al. [23].

2.4. Characterization of plant-based concretes

2.4.1. Mechanical proprieties

Mechanical compression test on concrete specimens was conducted after 60 days of setting with an electromechanical testing machine (MTS Criterion) with a 50 kN capacity. The tests were performed with the same protocol used in our previous work [23], with a loading rate of 5 mm/min. Cycles of loading/disloading were applied for 1%, 2% and 3% strain. The tests were conducted at 20°C and 50% relative humidity. For each mixture at least three specimens were tested (3 replicates). Samples are placed between two parallel plates and no surfacing of the sample is applied before the test. The Young's modulus was calculated on loading cycles and the deformation is relative to the initial height of the sample and the displacement of the upper plate. The compressive strength (σ_{max}) or the stress at 5% and 30% strain ($\sigma_{5\%}$, $\sigma_{30\%}$) was determined depending on the stress-strain behavior of concrete and used to compare the concretes. Results are presented via box plots which present the minimum and maximum values, the lower and upper quartiles, median, and mean values.

2.4.2. Thermal Properties

Thermal conductivity of concrete specimens was measured by means of a thermal apparatus (CT-meter FP2C-NeoTIM) using a hot linear wire probe (NF EN ISO 8894) which generate a heat flux by Joule effect and measure the rise in temperature by the sensor (50mm) between two identical samples ($\pi \times 5.5^2 \times 22$ cm^3). The test temperature was limited to 20°C; the heating time was taken as 400 s and the electrical power was 0.2 W. Prior to testing, every specimen was dried at 100°C then cooled for about one night at room temperature (20°C) in a tight plastic bag, in order to avoid any humidity intake during the

measurement. Tests were conducted at least six times for each formulation under the same conditions (20°C,50%HR).

2.4.3. The moisture buffer value

The moisture buffer value was measured according NORDTEST project method [43]. This value indicates the ability of hygroscopic materials to absorb or release moisture under dynamic conditions. it's corresponds to the amount of water vapor uptake or release by material per open surface area under daily cyclic variation of the surrounding relative humidity.

Samples were exposed to daily cyclic relative humidity variations: 8h exposure to 75% relative humidity followed by 16 h at low relative humidity exposure to 33% relative humidity at a constant temperature of 23°C using a WeissTechnik WKL150/10 climate test chamber. The MBV (moisture buffer value) was calculated by Eq. (7).

$$MBV = \frac{\Delta m}{A(HR_{high} - HR_{low})}$$

7

where Δm, is the average between the weight gain/loss during absorption/drying cycles [kg].

$RH_{high/low}$ are the high (75%) and low (33%) relative humidity [%].

A is the exposed surface area [m^2].

The thicknesses of samples were between 9 and 10 cm. The samples were sealed on all but one side with an aluminum foil tape and preconditioned at 23°C and 50% HR before the tests. The exposure surface area of materials was 3.14 x 25 cm^2. For each formulation, three samples were tested.

Specimens were weighed several times under 50% HR and 23°C conditions until the change in mass between the last three consecutive cycles was less than 5% of discrepancies.

2.4.4. SEM observations of concretes

For each sample, interfacial interactions between lime and aggregate were analyzed by ESEM (FEI Quanta 200). Microstructural analysis of the concretes was also conducted on compression tests specimens in order to highlight the structure of concretes such as the arrangement of vegetable particles and porosity in concretes.

3. Results And Discussion

3.1. Characterization of rice plant particles

3.1.1. Morphology

Figure 1, shows the cross-sections of rice husk (RH) and rice straw (RS) with different magnifications. Micrographs (Fig. 1.a) revealed a honeycombing and porous structure for rice straw. From the outside to the inside, it is formed of an epidermis (Ep), which has a concentrated layer of silica and other inorganic substances, xylem that contain vessels (Ve) and serve as capillaries for moisture sorption (water transport), phloem (PL) containing parenchyma cells (PC) which transports sugars, proteins and minerals, a pith characterized by largest parenchyma cells, and a lumen in the center. Although, morphology (Fig. 1.b) showed that rice husk is composed of an external epidermis characterized by a very particular morphology (convex-concave surface) rich in amorphous silica and an internal epidermis containing less silica. Between those components we can also observe a region of vascular bundles and parenchymal cells. The interior of the rice husk is made of cortex containing bundles of fibers, phloem and xylem. It can be seen that RH contains small pores along the cross-section with less variability in size, with a size range of 5–10 μm. However, these results are lower than those mentioned by Chabannes et al. [23, 44]. While, RS is characterized by a very porous structure with a random pore size distribution, the numbers of cell sizes and diameter continuously increase more and more towards the lumen of the straw particle. the average pore size for RS is in the range of 20–60 μm, and the average pore area varies from 250 to 950 μm^2.

3.1.2. Chemical composition

Table 2. shows the biochemical composition within rice plant particles obtained by the solvent extraction procedure. Rice husk (RH) and rice straw (RS) vary in chemical composition, however, the main components of the rice plant particles are cellulose, hemicelluloses, lignin, lipophilic extractives and ashes. Rice husk (RH) contains about 36% cellulose 22% hemicelluloses, 17% lignin, 8% lipophilic extractives and about 16% ash, which consists mainly of silica (45%). Compared to rice husk (RH), rice straw (RS) is higher in holocellulose (i.e. cellulose, hemicelluloses) content, this component is considered as very hydrophilic polysaccharide due to its high content of hydroxyl group. It should be kept in mind that the concentrations of these components depend strongly on the location of a particle on plant. Indeed, Jin et al[45], divided rice straw into fractions by morphological character (internodes, nodes, leaves sheath and blade) and investigated the chemical composition of different fractions of whole straw. Results reveal that leaves have larger cellulose fraction contents than either internodes or nodes.

Table 2
Chemical composition of plant rice aggregates

	Percentage of dry weight (%)	
Constituents	RH	RS
Cellulose	37 ± 3.1	40 ± 4.2
hemicelluloses	22 ± 4.1	22 ± 3.0
lignin	17 ± 3.7	11 ± 3.9
extractives	8 ± 3.5	15 ± 6.1
Ashes	16 ± 1.5	12 ± 2.3

3.1.3. Size and shape distribution

The morphological characteristics of rice straw particles (RS) and rice husk (RH) were compared based on image analysis. Results show that rice husk width varies from 0.5 to 3.2 mm and the maximum length is about 9.1 mm. In the case of rice straw particles, the width distribution varies from 1 mm to 11 mm and the length can reach up to 8 cm. Moreover, the average equivalent diameter is 3.5 mm for rice husk, and 15 mm for rice straw (Fig. 2).

In addition, the aspect ratio defined as the length on width ratio (L/W) is higher for rice straw aggregates (AR=10) and shows a higher standard deviation than rice husk (AR=5) which is linked to the heterogeneity of particles obtained by the manual cutting process (Fig. 3). Indeed, the PSD mainly depends on the production process (milling) and the quality of separation. Based on these results, it can be seen that rice husk has a near-spherical shape whereas rice straw has an elongated cylindrical shape. These characteristics must affect the microstructure (particles arrangement, density, and porosity) of concerts and thus its mechanical and hydrothermal proprieties.

3.1.4. Dry densities and porosities

The loose bulk density of the rice husk was in the range of 103 kg/m^3 which is 2 times greater than that of the rice straw RS. Indeed, compared to rice straw rice husk requires less volume at the same weight. This is surely linked to their boat-like shape, which must induce more voids (inter-granular porosity) between particles due to the imperfect rearrangement of these particles compared to rice straw that has a cylindrical shape. The very low bulk density of rice straw is justified by and its higher intra-granular (lumen). The loose bulk density of rice husk is close to the values reported in the literature [46], which is about 97 kg/m^3. Nevertheless, the bulk density of rice straw can vary depending on the different forms it may take. Thus, for straw bale, the loose bulk density varies from 20 to 40 kg/m^3[47], while, it's about 61 kg/m^3 for chopped rice straw (of about 5 cm pieces)[48] .

The absolute density measured with helium pycnometer was 1481 kg/m^3 for rice husk, this result meets the value found in the work of Chabannes et al. [46]. For the rice straw, the absolute density was 1373 kg/m^3, compared to the absolute density of wheat straw and barley straw (ranging from 865 to 871 kg/m^3) reported by Bouasker et al, [49], the absolute density of rice straw is much higher.

The difference in absolute density between the two kinds of aggregates used in this study is explained by the different chemical composition, especially to the content of ash, which, are rich in inorganic elements (Si, Mg...) characterized by a high atomic weight, in fact, rice straw contains less ash than rice husk.

In addition, the apparent density of a single particle was calculated based on its absolute density and its open porosity. Results show that a single rice husk has an apparent particle density, which is almost 2 times higher than that of rice straw. This is due to its lower intra-granular porosity as shown in Table 3. This results in a lower internal porosity but a higher inter-granular porosity for rice husk. These findings are in agreement with SEM micrographs presented in section (3.1.1), where a high rate of porosity and biggest pores were observed for rice straw.

Although RS have higher total porosity compared to RH (96% for RS and 93% for RH), this is related to the fact that rice straw has higher intra-granular porosity. It should be noted that the highly porous nature of rice straw and its low bulk density might play a very important role in improving the hydrothermal properties of rice straw concretes. The porosities measured in this study for rice husk are relatively close to those reported by Chabannes et al. [46].

Table 3
Densities and porosities of aggregates

	Rice husk	**Rice Straw**
	kg/m^3	
Bulk density ρ_b	103 ± 14.2	50 ± 8.5
Apparent density ρ_a (Estimated)	596.30	235.96
True density ρ_t	1481.27 ± 16.8	1373.6 ± 13.5
	%	
Open porosity $\eta_0 = 1 - \rho_a / \rho_t$	59.77	82.83
Inter-granular porosity $\eta_i = 1 - \rho_b / \rho_a$	82.62	78.59
Total porosity $\eta_t = 1 - \rho_b / \rho_t$	93.01	96.32

3.1.5. Water sensitivity of particles

The kinetic curve of water absorption tests is plotted in Fig. 4. Two distinct stages can be observed. A first phase which lasts 5 min characterized by a linear curve where a rapid weight increase occurs (Fick laws diffusion). During this phase the intake of water results from the capillary action (capillarity forces) attributed to the higher open porosity observed for plant aggregates and causes an almost instantaneous mass increase. The water absorption coefficient shows a significant difference between rice husk (RH = 77%) and rice straw particles (RS=187%), this is attributed to the largest pores in rice straw which seem to play a key role in their water absorption capacity and to water diffusion through plant cell. It should be kept in mind that natural aggregates have a strongly hydrophilic character, provided by their free hydroxyl groups mainly present in the cellulose, and hemicelluloses.

A second absorption stage (non-Fickian diffusion), slow and continuous follows a logarithmic law and occurs after five minutes of immersion up to saturation (48 h). As expected, both aggregates show a slower absorption kinetic at this stage. This behavior is attributed to changes in the microstructure of aggregates due to the presence of internal stresses related to the swelling and moisture absorption according to Brouard et al.[50]. RS can absorb up to 350% of its dry mass which is equivalent to 3,5 times its dry weight. Whereas, the water absorption coefficient for rice husk is only about 1.1 (WA= 110%). Indeed, the water absorption coefficient of rice husk has been assessed by Chabannes et al.[23] .The authors outline a water absorption rate of 120% for rice husk after 1h of immersion.

Additionally, in the case of rice husk (RH) the water absorption appears to stabilize and reach saturation stage after 120 min. While rice straw (RS) particles keep absorbing a less important amount of water before reaching equilibrium after 4h. This might depend on many parameters such as: the surface wettability of the vegetable particles, their chemical composition, the high porosity and the internal structure of these particles, which tends to reinforce the water absorption within rice straw (RS). The high internal porosity of the straw tends to enhance water diffusion within the aggregates, moreover, when considering the biochemical composition of aggregates, compared to rice husk, rice straw contains a high amount of hydrophilic components (i.e., cellulose and hemicelluloses) which contain hydroxyl reactive groups -OH and carboxyl groups -COOH. These groups can bound to free water molecules and then increase the hydrophilic character of straw particles.

It should be pointed out that the high water absorption during the first minutes might induce competition for water demand between binder and aggregates during manufacturing which impacts binder hydration, hence, disrupting the setting of the concretes, therefore natural aggregates must be wetted before the implementation of the binder. Nevertheless, in the long term saturated aggregates can pump the absorbed water to the binder, which may be particularly beneficial to the hydration process of the binder. This characteristic might affect the thermal and hygric properties of concretes.

3.2. Characterization of rice plant concretes

3.2.1. Dry densities

Once samples were removed from the mold, they were placed in an environment with stable conditions of temperature and relative humidity (23°C, 50% RH) for drying and carbonation. The variation of the specimen density with different RH/RS ratios was measured every 48 h, for 60 days. The dry densities after 2 months of the setting are highlighted in Table 4. it can be observed that density decreases linearly with increasing RH/RS ratio. This can be partially explained by the important porosity and the greater amount of water absorbed by straw particles. The difference in initial water content between rice husk and rice straw particles might confirm these findings. In fact, as the water content of RS was more important than in RH particles, higher evaporation of the initial water was observed in the rice straw concretes.

Additionally, it appears that the difference in dry density is also depending on both particles densities and granular stacking generated by mixing rice husk and rice straw, which might improve the compactness and lead in some way to the decrease of final density in concretes.

Table 4
Apparent densities of concretes before and after hydric stabilization

Mixtures	Fresh Apparent density (kg/m^3)	Dry Apparent density (kg/m^3)
100%RH	980	635 ± 15.3
33%RS	980	575 ± 10.5
50%RH	900	560 ± 12.4
66%RS	800	455 ± 9.3
100%RS	800	446 ± 8.7

The apparent density concretes decrease with increasing rice straw content, the highest density is obtained for concretes performed only with rice husk, it is about 635 kg/m^3, it significantly higher compared to the value obtained for concretes performed only with rice straw (446 kg/m^3). However, it should be noticed, that the fresh density of RH concrete was higher. The different densities of the two aggregates explain these finding, since the bulk density of RH is two time higher than that of RS, which results in a higher volume occupied by RS, compared to that of RH for the same mass. Also to the microstructure of concretes related to the orientation and the arrangement of particles under compaction performed during specimens manufacturing.

3.2.2. Porosities within concretes

Concretes are characterized by three different porosities: inter-granular porosity, which corresponds to the air gaps, left between several aggregate particles. intra-granular porosity, which corresponds to the pores inside the particles and inside the binder paste, and the total porosity, which corresponds to the addition of both types of porosity constituted from open and closed pores.

Porosities within concretes are plotted in Fig. 5. Results revealed that the total porosity increase by increasing rice straw content, which due to the high degree intra-granular porosity of rice straw as explained previously (see section 3.1.4), but also to its lower density. For instance, the total porosities of the two reference concretes (100%RH and 100%RS) are 80% for RS concrete, while, it is about 70% for RH concrete. However, the inter-granular porosity of RH concretes is higher than that of RS concretes. This is due to the higher apparent density and the shape of the rice husk. Furthermore, the lowest inter-granular porosity was observed for 50%RS combination; this might be related to the granular stacking and arrangement of natural particles in the concrete.

3.2.3. Microstructure observations at the particle / matrix interface

The scanning electronic microscopic images collected from the examination of the cross section of concretes are shown in Fig. 7. Results evidence the porous structure of concretes and highlight the pore's size diameter (voids) created between particles (inter-particles porosity). It can be observed that the porosity decreases with the RS/RH ratio and the pores diameter. These differences depend on the size of the particles, the morphology of particles, the RS/RH ratio and the orientation of particles due to the compaction process. That is why the RH concretes has a greater porosity, while RS presents low porosity and small pores. Yet, more pores, with different diameter are visible in the case of RH concretes (Fig. 6. (a)). It is clear that the compositions (33%RS, (Fig. 6. (b)), (50%RS, (Fig. 6. (c)) and (66%RS, (Fig. 6. (d)) are characterized by a low apparent porosity between particles. This can be explained by the particular morphology of the straw and orientation of particles, which put themselves in the perpendicular direction to the applied compaction when the particles are mechanically compacted during the manufacturing process, this might lead binder to fill pores between RH and RS particles. Furthermore, rice husk particles were also observed between rice straw particles (filling the pores) this might improve the compactness of concretes containing rice straw. On the contrary, to rice husks which are randomly oriented to three dimensions due to their particular geometry and size.

On the other hand, in the transition zone between particles and hardened lime, it appears that the straw particles are properly surrounded by the lime matrix compared to rice husk which might ultimately enhance the mechanical properties of concretes. These differences are explained by a higher roughness of the straw surface which is expected to improve mechanical interlocking by the creation of anchorage points with the lime binder.

3.2.4 Mechanical behavior of concretes

Figure 7. shows stress-strain curves of uniaxial compression of concretes, results show that rice husk concretes (100%RH) maintain a brittle behavior with maximum stress which passes through a maximum value, thus making it easier to determine strength or resistance. On the other hand, concretes containing rice straw particles have a different behavior they show a very ductile behavior since any collapses have been observed in the case of these concretes. These concretes have a large deformation capacity. As a consequence, to compare the concretes and investigate the impact of rice straw content on mechanical

characteristics, stress at 5% strain close to the end of the linear elastic area and 30% strain in the strain hardening area values have been selected. In addition, the young's modulus (E) was calculated on loading cycles which is significantly different from the apparent one determined by the slope of the linear part of the stress-strain curve.

Concretes containing rice straw particles show a very ductile behavior, the stress-strain curve can be divided into three main regions: a quasi-elastic linear stage when the concrete was first loaded, a quasi-linear hardening phase when the load increases almost linearly with the increase of deformation. in this region, the hollow straw tubes start to collapse and then a densification stage occurs as the concretes become more compact, thus, concretes become harder to crush and can absorb a large amount of energy without total structural failure. This is similarly to results reported in the literature [51–54].This highly viscous behavior is attributed to straw particles[55–57].

On the other hand, rice husk concretes (100%RH) show a very brittle behavior; the stress-strain curve shows abrupt failure at 0.33 MPa (median value), these concretes have the highest elastic modulus which is about 55.2 MPa (median value). On the opposite, concretes prepared with straw particles continue to be deformed while undergoing significant deformation (up to 50%). Results indicate that rice straw generates greater deformability and leads to the increase in ductility of concretes. This behavior might be attributed to compactness related to the packing of particles and the filling of inter-particles porosity under a high stress. Rice husk could be inserted between the large rice straw particles and thus increase the compactness of the concretes.

Furthermore, results show that the strain decreases with RS/RH ratio increase. In fact, 33%RS concretes show the highest stress at both 5% and 30% strain, the corresponding strain value is 0.21 and 1.11 MPa, respectively. It can be observed that elastic modulus and resistance (stress at 5 and 30%) are directly proportional to the straw content (Fig. 8). Indeed, the addition of the rice straw decreases the resistance of the concretes and reduces its rigidity. It can be observed that the rigidity of the concretes significantly decreased about 45% when 33% of rice straw was added.

This might be due to the higher water absorption of the RS that decreases the hydration of the hydraulic lime and results in low strength. it can be also linked to the quality of the interfacial adhesion which is primarily related to the size of particles and their topography. A better interfacial bonding occurs between the small particles and the lime matrix (RH). In effect, it's well known that interface/interphase plays a key role in load transfer [16]. Furthermore, it was observed that concretes containing rice straw particles cannot be crushed but can only be compacted under loading which only causes the deterioration of the micro-tubes of straw and lead to further densification of the concretes (Fig. 9). It was observed that concretes tend to return to their initial shape after deformation (end of compression test).

3.2.5. Thermal conductivity

The thermal conductivity of concretes was measured at (20°C; 50%RH) in order to characterize the thermal behavior of the concretes. At least six measurements were carried out for each formulation, thus

results are presented with mean, minimum, and maximum values due to the dispersion of the values. Fig. 10. (a) reports the variation of thermal conductivity of dry concretes for different aggregates. So, as it was shown in Fig. 11.a. The rice husk concretes 100%RH present the highest thermal conductivity 115 mW/(m K). These higher thermal conductivity values are related to the higher density of the rice husk concretes and are in agreement with the values found in the literature. Actually, In previous work Chabannes et al [23]. studied the thermal conductivity of rice husk and hemp concrete manufactured by compacting, they give thermal conductivity values of 119 and 108 mW/(m K) when the densities are respectively 637 and 459 kg/m^3.

Furthermore, results show that thermal conductivity tends to decrease with the amount of the straw RS, Indeed, the thermal conductivities of 33%RS, 66%RS and 100%RS were 101, 84 and 98 mW/(m.K), respectively. The density and the porosity of these concrete, which decreases with the quantity of straw, can explain this. However, for the composition (50%RS) is not the same trend, it gave an average thermal conductivity of 111 mW/(m.K) despite its low density. It's mainly due to its lowest intra-granular porosity, which is related to the geometric arrangement and random distribution of the particles used for this formulation, which might engender a complex microstructure. This may indicate that conductivity is more impacted by porosity than density. 66%RS and 100% RS can be qualified as insulating materials since their thermal conductivity is < 0.1 W. $m^{-1}.K^{-1}$ (according to French regulation) [58, 59].
it seems that density and thermal conductivity have a linear tendency. Results underline that thermal conductivity increases linearly with density (Fig. 10. (b)), indeed, the lighter the concrete, the lower and its thermal conductivity. However, the density of concretes depends strongly on rice straw content, it decreases by increasing the content of rice straw. This is attributed to the high porosity and lower bulk density of rice straw. Furthermore, these finding shows that porosity (voids' ratio) within the concrete plays a key role in thermal performances. In fact, pores can be filled with air which leads to lower thermal conductivity. This is in correlation with results previously reported by Collet et al .[16].

3.2.6. Moisture buffer value

The effect of rice straw content on hygric properties has been assessed by Moisture Buffer Value (MBV) measurements. The Moisture Buffer Value can be used to evaluate concretes ability to absorb and release moisture (moderate ambient relative humidity variations).

Figure 11. (a) present the MBV values of all concretes calculated for three last cycles, when the steady-state is reached. From an overall observation of the moisture buffer values MBV, it can be deduced that the MBV varies greatly depending on the samples composition (constituent ratio), which results in differences in density and porous structure.

Results underline that increasing the percentage of straw enhances the MBV. Indeed, the increase in the RS/RH ratio leads to a higher MBV. It is evident that the moisture buffering capacity of concretes strongly depends on the content of straw particles. Compositions, (100%RS) and (66%RS) exhibit the first two performances with moisture buffering values respectively: 2.1 and 1.87 g/m^2. %RH, However, the MBV value of (100%RH - reference concrete) is the lowest with 1.2 g/m^2. %RH. Based on the classification

established by the NORDTEST Project, the first noticed point is that 100%RS concretes are considered as excellent hygric regulators whereas all other concretes demonstrate good moisture buffering capacity. Comparing to literature, moisture buffer values obtained in this study are higher than those of hemp plaster [60], but are lower than values met in literature for rape straw concrete (2.6 g/m^2. %RH)[25], and flax concretes (2.03-2.81 g/m^2. %RH)[61]. the densities of these latter vary from 400 to 750 kg/m^3.

The obtained results could be attributed to the characteristics of rice straw, such as its high moisture adsorption and restitution capacity and its high interconnected porosity, and the pore sizes, which allow moisture transfer and storage. Therefore, the increase in the RS/RH ratio leads to a higher MBV value and allows reaching better hygroscopic performances.

As it can be seen in Fig. 11. (b), a high correlation between the increase of MBV and the increase of porosity of concretes was underlined. The relationship between MBV and total porosity shows that both the internal structure of concretes and intra-granular porosity of particles and binder plays a key role in the hygric performances of the materials. In fact, concretes might store water in their different pores, which ranged approximately from the µm-mm for intra-particle porosity to the mm-cm for inter-particles porosity.

4. Conclusion

The presented work provides a sustainable use option for rice culture waste. By development of an environmentally friendly material made from rice plant by-products. Moreover, this work analyzed the mechanical and hydrothermal proprieties of a new bio-based concrete containing rice husk and rice straw particles with varied rice straw/rice husk ratio. Globally, concrete behavior is mainly governed by the quantity of rice straw particles constituting the material. However, the following conclusions can be drawn from the present work:

- The physical characterization shows that rice straw particles have a porous structure and a higher aspect ratio (L/d) with a high degree of total and intra-granular porosity. When compared to rice husk particles. Also, chemical analysis revealed that rice straw contains high degree of cellulose and hemicelluloses. This gives them a high water absorption capacity (hydrophilic property).
- SEM observation of concretes showed good adhesion between the plant aggregates and binder, which validated the compatibility of both materials.
- The porosity of concretes was increased gradually when the proportion of straw was increased; on the other hand, the increase in the amount of rice straw particles leads to a reduction in concretes density.
- Concerning the thermal analysis, the thermal conductivity was directly proportional to density and porosity. However, it was shown that porosity is the property that has a greater impact on thermal conductivity. Furthermore, we concluded that the higher the rice straw (RS) content, the lower the thermal conductivity of concretes.

- Concerning the hygric properties, it was shown that MBV increases with increasing rice straw content in the material. Compared to other concretes, concrete performed with rice straw only appears as relevant and shows the highest MBV value of approximately 2.2 g/m^2. % RH. The MBV of concretes is governed by the voids presented in samples. However, the hygric properties of concrete should be explored in detail.
- The compressive strength and young modulus of concrete decrease with increasing the content of rice straw in the concretes. A high straw content induces an increase in porosity, which ultimately results in poor mechanical performance. Furthermore, results indicate that the deformation does not lead to the fracture of concretes containing rice straw, but induces a continuous increase of stress, these materials enable the storing of high quantity of energy.

Declarations

Statements & Declarations

- We confirm that the manuscript has been read and approved by all named authors.

- We confirm that the order of authors listed in the manuscript has been approved by all named authors.

- We confirm that this manuscript has not been published elsewhere and is not under consideration by another journal.

- We confirm that we have given due consideration to the protection of intellectual property associated with this work and that there are no impediments to publication, including the timing of publication, with respect to intellectual property. In so doing we confirm that we have followed the regulations of our institutions concerning intellectual property.

- We wish to confirm that there are no known conflicts of interest associated with this publication and there has been no significant financial support for this work that could have influenced its outcome.

- All authors have approved the manuscript and agree with its submission to Waste and Biomass Valorization .

Competing Interests

The authors have no relevant financial or non-financial interests to disclose

CRediT authorship contribution statement

Youssef El Moussi : Conceptualization, Data curation, Formal analysis, Investigation, Visualization, Writing - original draft

Laurent CLERC : Conceptualization, Methodology , Supervision

Jean-Charles BENEZET : Project administration, Methodology, Supervision.

Data Availability Statement

The authors confirm that the datasets generated and/or analysed during the current study are available within the article. Raw data that support the findings of this study are available from the corresponding author, upon reasonable request

Acknowledgments

The authors would like to thank Jean-Claude ROUX (IMT Mines Alès) for SEM experiments, and Alain DIAZ, and Alexandre CHERON (IMT Mines Alès) for their technical support.

References

[1] A. S. Ahmad *et al.*, “A review on applications of ANN and SVM for building electrical energy consumption forecasting,” *Renew. Sustain. Energy Rev.*, vol. 33, pp. 102–109, 2014, doi: 10.1016/j.rser.2014.01.069.

[2] K. Amasyali and N. M. El-Gohary, “A review of data-driven building energy consumption prediction studies,” *Renew. Sustain. Energy Rev.*, vol. 81, no. March 2017, pp. 1192–1205, 2018, doi: 10.1016/j.rser.2017.04.095.

[3] Bosseboeuf et al., “Energy Efficiency Trends and Policies in the Household and Tertiary Sectors : An Analysis Based on the ODYSSEE and MURE Databases,” no. June, pp. 1–97, 2015, doi: DOI 10.1089/pho.2012.3369.

[4] X. Cao, X. Dai, and J. Liu, “Building energy-consumption status worldwide and the state-of-the-art technologies for zero-energy buildings during the past decade,” *Energy Build.*, vol. 128, pp. 198–213, 2016, doi: 10.1016/j.enbuild.2016.06.089.

[5] O. Kaynakli, “A review of the economical and optimum thermal insulation thickness for building applications,” *Renew. Sustain. Energy Rev.*, vol. 16, no. 1, pp. 415–425, 2012, doi: 10.1016/j.rser.2011.08.006.

[6] L. Yan, B. Kasal, and L. Huang, “A review of recent research on the use of cellulosic fi bres , their fi bre fabric reinforced cementitious , geo-polymer and polymer composites in civil engineering,” *Compos. Part B*, vol. 92, pp. 94–132, 2016, doi: 10.1016/j.compositesb.2016.02.002.

[7] F. Asdrubali, F. D'Alessandro, and S. Schiavoni, "A review of unconventional sustainable building insulation materials," *Sustain. Mater. Technol.*, vol. 4, no. 2015, pp. 1–17, 2015, doi: 10.1016/j.susmat.2015.05.002.

[8] F. Collet, M. Bart, L. Serres, and J. Miriel, "Porous structure and water vapour sorption of hemp-based materials," vol. 22, pp. 1271–1280, 2008, doi: 10.1016/j.conbuildmat.2007.01.018.

[9] M. Palumbo, A. M. Lacasta, N. Holcroft, A. Shea, and P. Walker, "Determination of hygrothermal parameters of experimental and commercial bio-based insulation materials," *Constr. Build. Mater.*, vol. 124, pp. 269–275, 2016, doi: 10.1016/j.conbuildmat.2016.07.106.

[10] P. Strandberg-de Bruijn and P. Johansson, "Moisture transport properties of lime-hemp concrete determined over the complete moisture range," *Biosyst. Eng.*, vol. 122, pp. 31–41, 2014, doi: 10.1016/j.biosystemseng.2014.03.001.

[11] S. Pretot, F. Collet, and C. Garnier, "Life cycle assessment of a hemp concrete wall: Impact of thickness and coating," *Build. Environ.*, vol. 72, pp. 223–231, 2014, doi: 10.1016/j.buildenv.2013.11.010.

[12] F. Pittau, F. Krause, G. Lumia, and G. Habert, "Fast-growing bio-based materials as an opportunity for storing carbon in exterior walls," *Build. Environ.*, vol. 129, no. August 2017, pp. 117–129, 2018, doi: 10.1016/j.buildenv.2017.12.006.

[13] P. M. Boutin, C. Flamin, S. Quinton, and G. Gosse, *Analyse du cycle de vie d'un mur en béton de chanvre banché sur ossature bois*. 2005.

[14] K. Ip and A. Miller, "Life cycle greenhouse gas emissions of hemp-lime wall constructions in the UK," *Resour. Conserv. Recycl.*, vol. 69, pp. 1–9, 2012, doi: 10.1016/j.resconrec.2012.09.001.

[15] C. Niyigena *et al.*, "Variability of the mechanical properties of hemp concrete," *Mater. Today Commun.*, vol. 7, pp. 122–133, 2016, doi: 10.1016/j.mtcomm.2016.03.003.

[16] F. Collet and S. Pretot, "Thermal conductivity of hemp concretes: Variation with formulation, density and water content," *Constr. Build. Mater.*, vol. 65, pp. 612–619, 2014, doi: 10.1016/j.conbuildmat.2014.05.039.

[17] Y. Diquélou, E. Gourlay, L. Arnaud, and B. Kurek, "Influence of binder characteristics on the setting and hardening of hemp lightweight concrete," *Constr. Build. Mater.*, vol. 112, pp. 506–517, 2016, doi: 10.1016/j.conbuildmat.2016.02.138.

[18] V. Nozahic and S. Amziane, "Influence of sunflower aggregates surface treatments on physical properties and adhesion with a mineral binder," *Compos. Part A Appl. Sci. Manuf.*, vol. 43, no. 11, pp. 1837–1849, 2012, doi: 10.1016/j.compositesa.2012.07.011.

[19] M. Chabannes, V. Nozahic, and S. Amziane, “Design and multi-physical properties of a new insulating concrete using sunflower stem aggregates and eco-friendly binders,” *Mater. Struct. Constr.*, vol. 48, no. 6, pp. 1815–1829, 2015, doi: 10.1617/s11527-014-0276-9.

[20] M. Rahim *et al.*, “Characterization of flax lime and hemp lime concretes: Hygric properties and moisture buffer capacity,” *Energy Build.*, vol. 88, pp. 91–99, 2015, doi: 10.1016/j.enbuild.2014.11.043.

[21] M. Chabannes, E. Garcia-diaz, L. Clerc, and J. Bénézet, “Effect of curing conditions and Ca (OH) 2 - treated aggregates on mechanical properties of rice husk and hemp concretes using a lime-based binder,” vol. 102, pp. 821–833, 2016, doi: 10.1016/j.conbuildmat.2015.10.206.

[22] M. Chabannes, E. Garcia-diaz, L. Clerc, and J. Bénézet, “Studying the hardening and mechanical performances of rice husk and hemp-based building materials cured under natural and accelerated carbonation,” *Constr. Build. Mater.*, vol. 94, pp. 105–115, 2015, doi: 10.1016/j.conbuildmat.2015.06.032.

[23] M. Chabannes, J. Bénézet, L. Clerc, and E. Garcia-diaz, “Use of raw rice husk as natural aggregate in a lightweight insulating concrete : An innovative application,” *Constr. Build. Mater.*, vol. 70, pp. 428–438, 2014, doi: 10.1016/j.conbuildmat.2014.07.025.

[24] V. Nozahic, S. Amziane, G. Torrent, K. Saïdi, and H. De Baynast, “Design of green concrete made of plant-derived aggregates and a pumice-lime binder,” *Cem. Concr. Compos.*, vol. 34, no. 2, pp. 231–241, 2012, doi: 10.1016/j.cemconcomp.2011.09.002.

[25] M. Rahim, O. Douzane, A. D. Tran Le, G. Promis, and T. Langlet, “Characterization and comparison of hygric properties of rape straw concrete and hemp concrete,” *Constr. Build. Mater.*, vol. 102, pp. 679–687, 2016, doi: 10.1016/j.conbuildmat.2015.11.021.

[26] N. Belayachi, M. Bouasker, D. Hoxha, and M. Al-Mukhtar, “Thermo-mechanical behaviour of an innovant straw lime composite for thermal insulation applications,” *Appl. Mech. Mater.*, vol. 390, no. youssef, pp. 542–546, 2013, doi: 10.4028/www.scientific.net/AMM.390.542.

[27] M. Labat, C. Magniont, N. Oudhof, and J. E. Aubert, “From the experimental characterization of the hygrothermal properties of straw-clay mixtures to the numerical assessment of their buffering potential,” *Build. Environ.*, vol. 97, pp. 69–81, 2016, doi: 10.1016/j.buildenv.2015.12.004.

[28] B. Belhadj, M. Bederina, N. Montrelay, J. Houessou, and M. Quéneudec, “Effect of substitution of wood shavings by barley straws on the physico-mechanical properties of lightweight sand concrete,” *Constr. Build. Mater.*, vol. 66, pp. 247–258, 2014, doi: 10.1016/j.conbuildmat.2014.05.090.

[29] B. Belhadj, M. Bederina, Z. Makhloufi, R. M. Dheilly, N. Montrelay, and M. Quéneudéc, “Contribution to the development of a sand concrete lightened by the addition of barley straws,” *Constr. Build. Mater.*, vol. 113, pp. 513–522, 2016, doi: 10.1016/j.conbuildmat.2016.03.067.

[30] X. Chen, X. Shi, J. Zhou, Z. Yu, and P. Huang, “Determination of mechanical, flowability, and microstructural properties of cemented tailings backfill containing rice straw,” *Constr. Build. Mater.*, vol. 246, p. 118520, 2020, doi: 10.1016/j.conbuildmat.2020.118520.

[31] J. Roselló, L. Soriano, M. P. Santamarina, J. L. Akasaki, J. Monzó, and J. Payá, “Rice straw ashA potential pozzolanic supplementary material for cementing systems,” *Ind. Crops Prod.*, vol. 103, pp. 39–50, 2017, doi: 10.1016/j.indcrop.2017.03.030.

[32] B. Gadde, S. Bonnet, C. Menke, and S. Garivait, “Air pollutant emissions from rice straw open field burning in India, Thailand and the Philippines,” *Environ. Pollut.*, vol. 157, no. 5, pp. 1554–1558, 2009, doi: 10.1016/j.envpol.2009.01.004.

[33] R. R. Romasanta *et al.*, “How does burning of rice straw affect CH4 and N2O emissions? A comparative experiment of different on-field straw management practices,” *Agric. Ecosyst. Environ.*, vol. 239, pp. 143–153, 2017, doi: 10.1016/j.agee.2016.12.042.

[34] A. Singh and P. Basak, “Economic and environmental evaluation of rice straw processing technologies for energy generation: A case study of Punjab, India,” *J. Clean. Prod.*, vol. 212, pp. 343–352, 2019, doi: 10.1016/j.jclepro.2018.12.033.

[35] J. Page, M. Sonebi, and S. Amziane, “Design and multi-physical properties of a new hybrid hemp-flax composite material,” *Constr. Build. Mater.*, vol. 139, pp. 502–512, 2017, doi: 10.1016/j.conbuildmat.2016.12.037.

[36] M. Fernández Bertos, S. J. R. Simons, C. D. Hills, and P. J. Carey, “A review of accelerated carbonation technology in the treatment of cement-based materials and sequestration of CO2,” *J. Hazard. Mater.*, vol. 112, no. 3, pp. 193–205, 2004, doi: 10.1016/j.jhazmat.2004.04.019.

[37] B. Mazian, A. Bergeret, J. C. Benezet, and L. Malhautier, “Influence of field retting duration on the biochemical, microstructural, thermal and mechanical properties of hemp fibres harvested at the beginning of flowering,” *Ind. Crops Prod.*, vol. 116, no. January, pp. 170–181, 2018, doi: 10.1016/j.indcrop.2018.02.062.

[38] T. Phuong, T. Tran, J. Bénézet, and A. Bergeret, “Rice and Einkorn wheat husks reinforced poly (lactic acid) (PLA) biocomposites : Effects of alkaline and silane surface treatments of husks,” *Ind. Crop. Prod.*, vol. 58, pp. 111–124, 2014, doi: 10.1016/j.indcrop.2014.04.012.

[39] J. Acera Fernández *et al.*, “Role of flax cell wall components on the microstructure and transverse mechanical behaviour of flax fabrics reinforced epoxy biocomposites,” *Ind. Crops Prod.*, vol. 85, pp. 93–108, 2016, doi: 10.1016/j.indcrop.2016.02.047.

[40] S. Amziane, F. Collet, M. Lawrence, C. Magniont, V. Picandet, and M. Sonebi, “Recommendation of the RILEM TC 236-BBM: characterisation testing of hemp shiv to determine the initial water content, water

absorption, dry density, particle size distribution and thermal conductivity," *Mater. Struct. Constr.*, vol. 50, no. 3, pp. 1–11, 2017, doi: 10.1617/s11527-017-1029-3.

[41] M. Viel, F. Collet, and C. Lanos, "Development and characterization of thermal insulation materials from renewable resources," *Constr. Build. Mater.*, vol. 214, no. x, pp. 685–697, 2019, doi: 10.1016/j.conbuildmat.2019.04.139.

[42] M. Chabannes, E. Garcia-Diaz, J. Bénézet, and L. Clerc, *Lime Hemp and Rice Husk- Based Concretes for Building Envelopes*. SPRINGER BRIEFS IN MOLECULAR SCIENCE, 2018.

[43] C. Rode, *Moisture Buffering of Building Materials Department of Civil Engineering Technical University of Denmark*. 2005.

[44] B. D. Park, S. Gon Wi, K. Ho Lee, A. P. Singh, T. H. Yoon, and Y. Soo Kim, "Characterization of anatomical features and silica distribution in rice husk using microscopic and micro-analytical techniques," *Biomass and Bioenergy*, vol. 25, no. 3, pp. 319–327, 2003, doi: 10.1016/S0961-9534(03)00014-X.

[45] S. Jin and H. Chen, "Structural properties and enzymatic hydrolysis of rice straw," *Process Biochem.*, vol. 41, no. 6, pp. 1261–1264, 2006, doi: 10.1016/j.procbio.2005.12.022.

[46] M. Chabannes, F. Becquart, E. Garcia-Diaz, N. E. Abriak, and L. Clerc, "Experimental investigation of the shear behaviour of hemp and rice husk-based concretes using triaxial compression," *Constr. Build. Mater.*, vol. 143, pp. 621–632, 2017, doi: 10.1016/j.conbuildmat.2017.03.148.

[47] F. Kargbo, J. Xing, and Y. Zhang, "Property analysis and pretreatment of rice straw for energy use in grain drying: A review," *Agric. Biol. J. North Am.*, vol. 1, no. 3, pp. 195–200, 2010, doi: 10.5251/abjna.2010.1.3.195.200.

[48] X. Chen *et al.*, "Enhancing methane production from rice straw by extrusion pretreatment," *Appl. Energy*, vol. 122, pp. 34–41, 2014, doi: 10.1016/j.apenergy.2014.01.076.

[49] M. Bouasker, N. Belayachi, D. Hoxha, and M. Al-mukhtar, "Physical Characterization of Natural Straw Fibers as Aggregates for Construction Materials Applications," pp. 3034–3048, 2014, doi: 10.3390/ma7043034.

[50] Y. Brouard, N. Belayachi, D. Hoxha, N. Ranganathan, and S. Méo, "Mechanical and hygrothermal behavior of clay – Sunflower (Helianthus annuus) and rape straw (Brassica napus) plaster bio-composites for building insulation," *Constr. Build. Mater.*, vol. 161, pp. 196–207, 2018, doi: 10.1016/j.conbuildmat.2017.11.140.

[51] T. Nguyen *et al.*, "Influence of compactness and hemp hurd characteristics on the mechanical properties of lime and hemp concrete Influence of compactness and hemp hurd characteristics on the mechanical properties of lime and hemp concrete," vol. 8189, 2011, doi: 10.3166/EJECE.13.1039-1050.

[52] A. T. Le, A. Gacoin, A. Li, T. H. Mai, and N. El Wakil, “Influence of various starch/hemp mixtures on mechanical and acoustical behavior of starch-hemp composite materials,” *Compos. Part B Eng.*, vol. 75, pp. 201–211, 2015, doi: 10.1016/j.compositesb.2015.01.038.

[53] R. Walker, S. Pavia, and R. Mitchell, “Mechanical properties and durability of hemp-lime concretes,” *Constr. Build. Mater.*, vol. 61, pp. 340–348, 2014, doi: 10.1016/j.conbuildmat.2014.02.065.

[54] N. Belayachi, D. Hoxha, and M. Slaimia, “Impact of accelerated climatic aging on the behavior of gypsum plaster-straw material for building thermal insulation,” *Constr. Build. Mater.*, vol. 125, pp. 912–918, 2016, doi: 10.1016/j.conbuildmat.2016.08.120.

[55] M. Maraldi, L. Molari, N. Regazzi, and G. Molari, “Method for the characterisation of the mechanical behaviour of straw bales,” *Biosyst. Eng.*, vol. 151, pp. 141–151, 2016, doi: 10.1016/j.biosystemseng.2016.09.003.

[56] M. Maraldi, L. Molari, N. Regazzi, and G. Molari, “Analysis of the parameters affecting the mechanical behaviour of straw bales under compression,” *Biosyst. Eng.*, vol. 160, pp. 179–193, 2017, doi: 10.1016/j.biosystemseng.2017.06.007.

[57] T. Lecompte and A. Le Duigou, “Mechanics of straw bales for building applications,” *J. Build. Eng.*, vol. 9, no. June 2016, pp. 84–90, 2017, doi: 10.1016/j.jobe.2016.12.001.

[58] R. Muthuraj, C. Lacoste, P. Lacroix, and A. Bergeret, “Sustainable thermal insulation biocomposites from rice husk, wheat husk, wood fibers and textile waste fibers: Elaboration and performances evaluation,” *Ind. Crops Prod.*, vol. 135, no. April, pp. 238–245, 2019, doi: 10.1016/j.indcrop.2019.04.053.

[59] N. Mati-Baouche *et al.*, “Mechanical, thermal and acoustical characterizations of an insulating bio-based composite made from sunflower stalks particles and chitosan,” *Ind. Crops Prod.*, vol. 58, pp. 244–250, 2014, doi: 10.1016/j.indcrop.2014.04.022.

[60] F. Collet and S. Pretot, “Experimental investigation of moisture buffering capacity of sprayed hemp concrete,” *Constr. Build. Mater.*, vol. 36, pp. 58–65, 2012, doi: 10.1016/j.conbuildmat.2012.04.139.

[61] F. Benmahiddine, R. Cherif, F. Bennai, R. Belarbi, A. Tahakourt, and K. Abahri, “Effect of flax shives content and size on the hygrothermal and mechanical properties of flax concrete,” *Constr. Build. Mater.*, vol. 262, p. 120077, 2020, doi: 10.1016/j.conbuildmat.2020.120077.

Figures

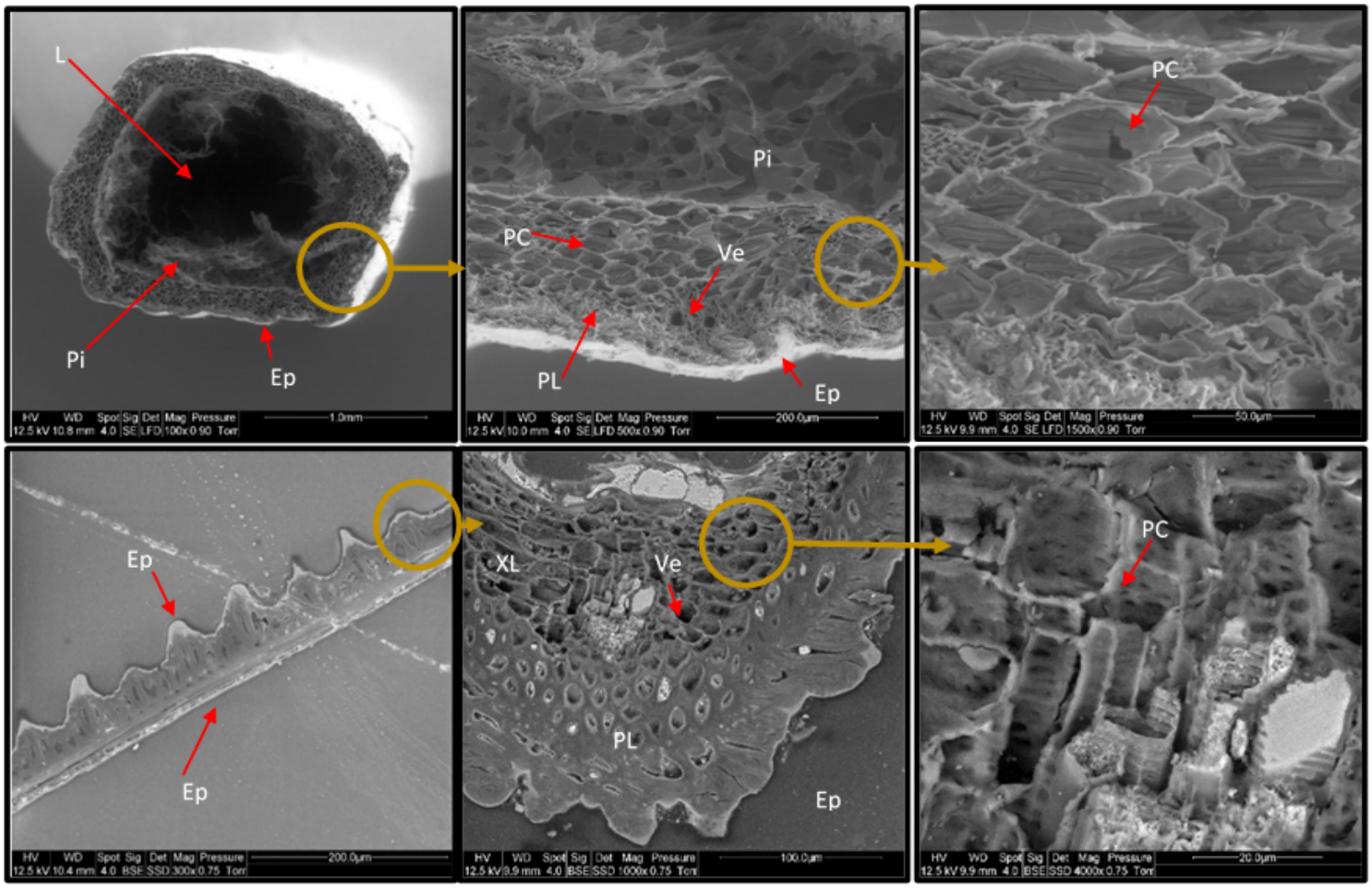

Figure 1

SEM Micrograph of cross sections of (a) rice straw RS ;(b) rice husk RH (Ep: epidermis, PL: phloem, PC: parenchyma cell, XL: xylem, Ve: vessel, L: lumen, and Pi: pith)

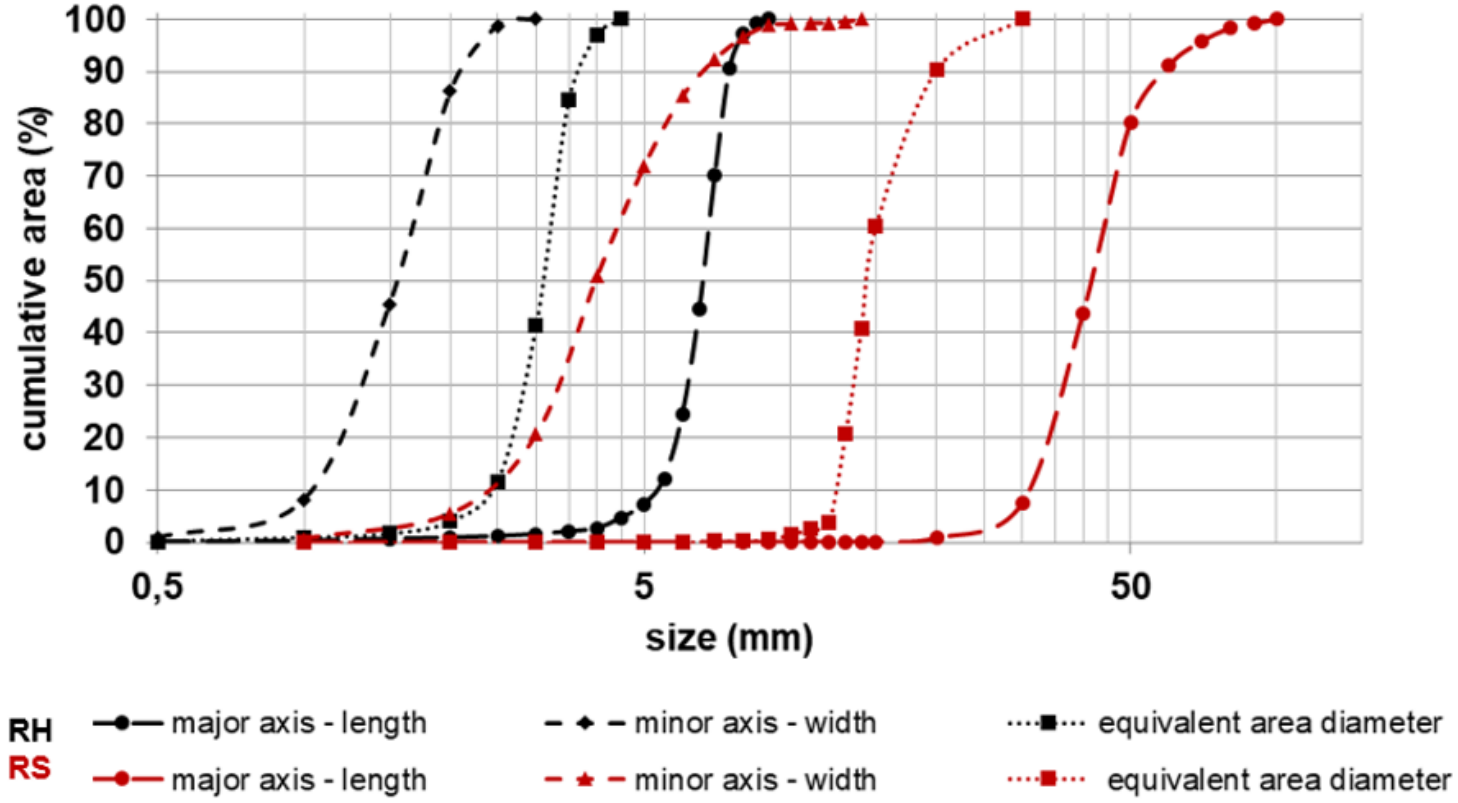

Figure 2

Granulometric distribution of RH, and RS aggregates

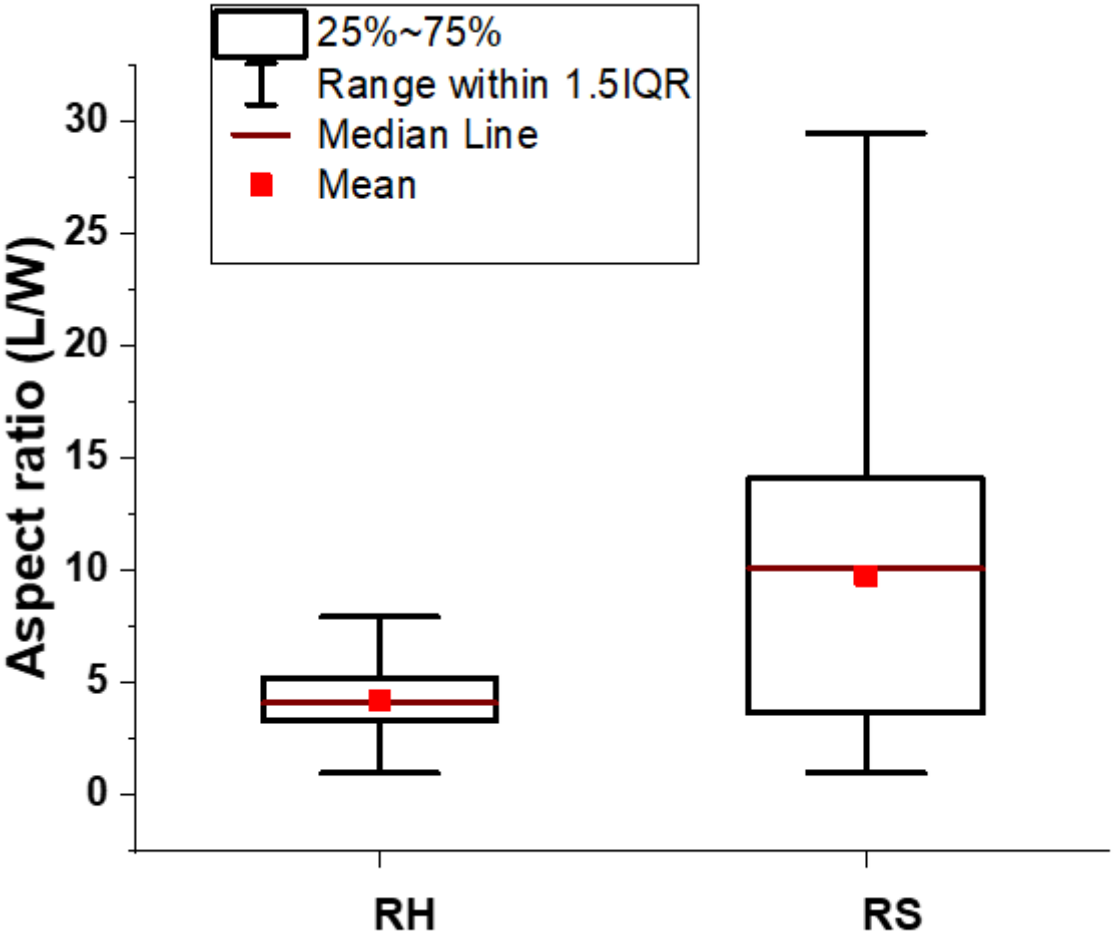

Figure 3

box plots of particles aspect ratio distributions

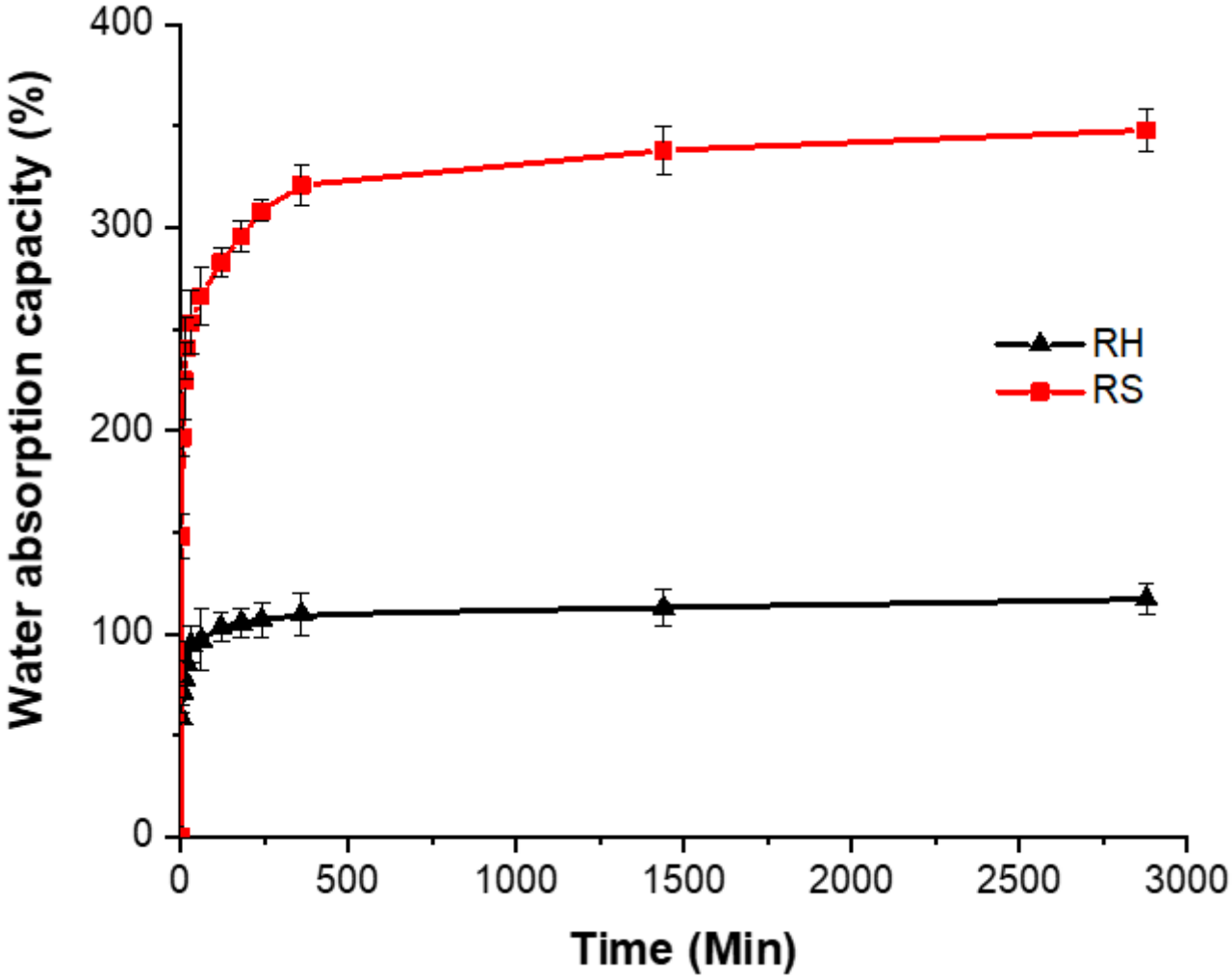

Figure 4

water absorption of rice husk and rice straw aggregates

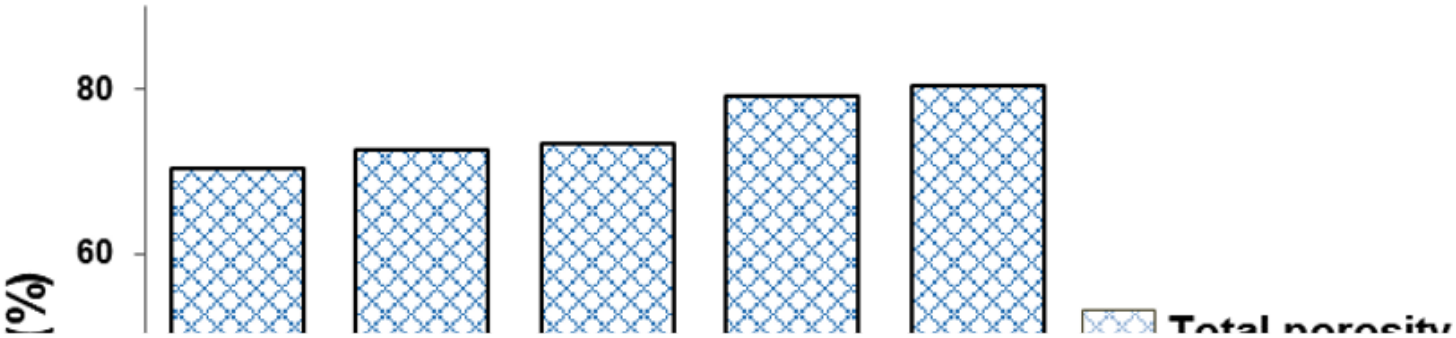

Figure 5

Porosities of husk/straw concretes

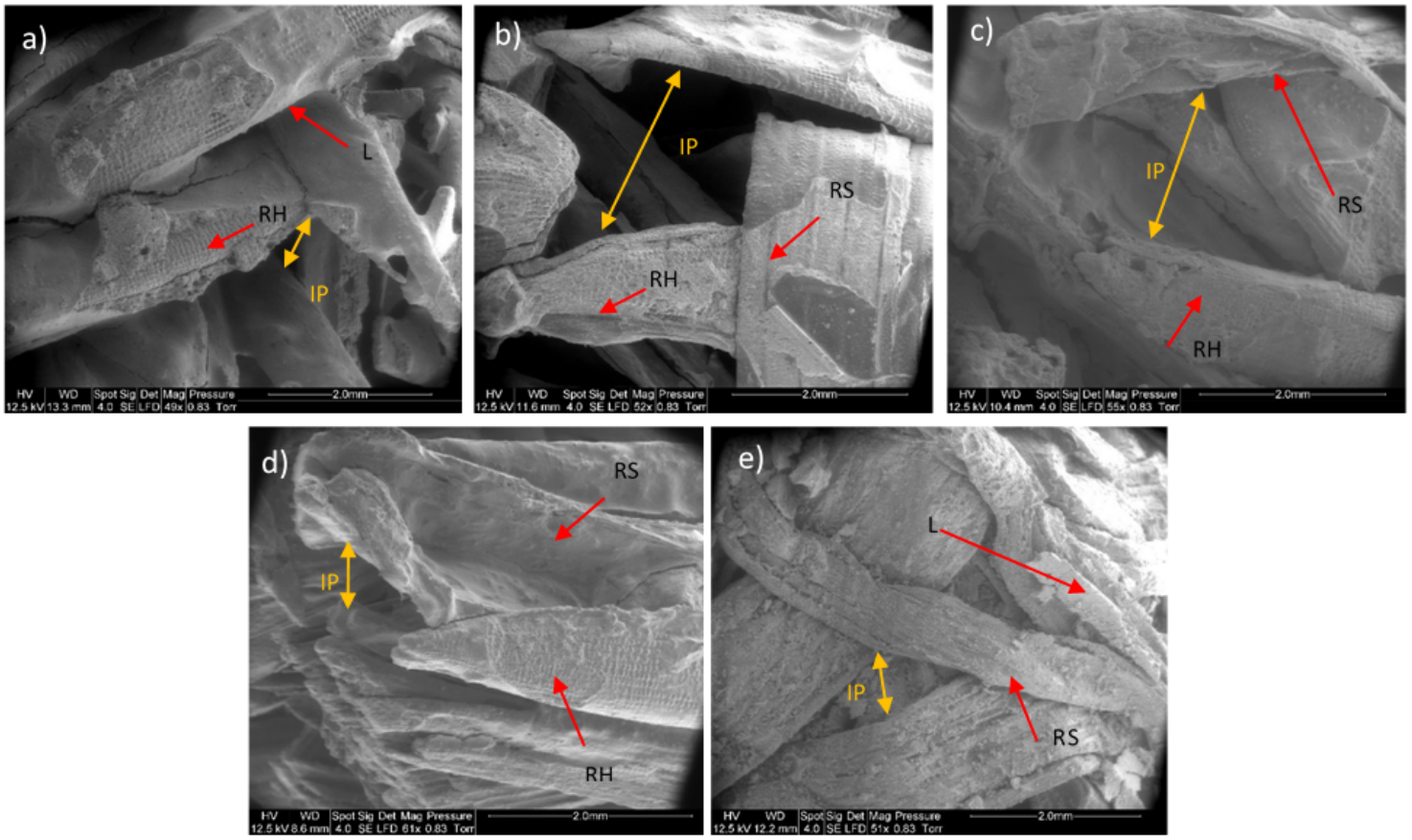

Figure 6

Micrographs of husk/straw concretes (a) 100% RH, (b) 33% RS, (c) - 50% RS, (d) 66% RS, (e) 100%RS (RS: rice straw, RH: rice husk, L: lime, IP: inter-granular porosity)

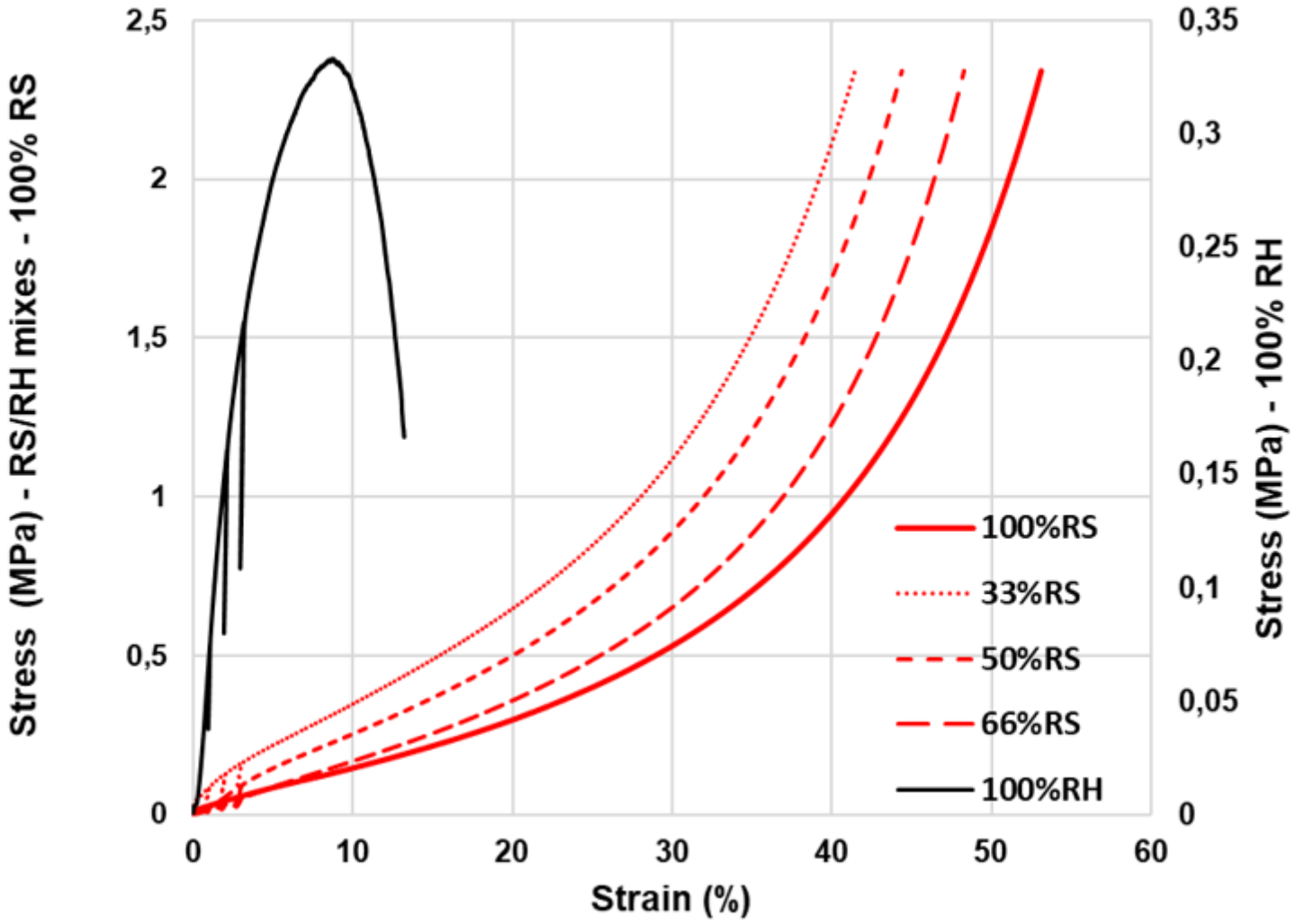

Figure 7

Uniaxial compression stress-strain curves for all mixtures of rice plant particles-lime concretes specimens after 60 days of setting.

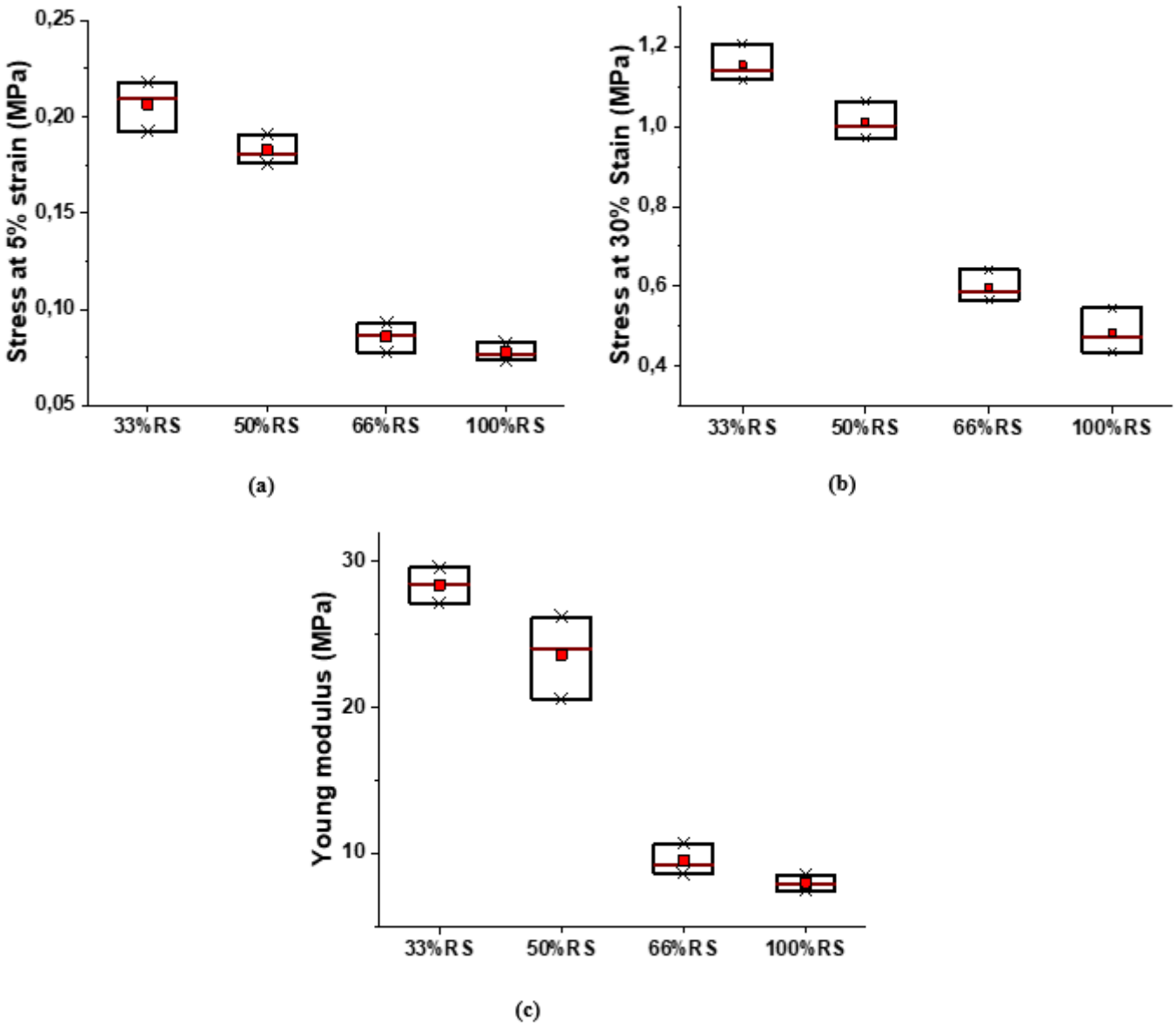

Figure 8

Effect of rice straw on compression properties of concretes: (a) Stress at 5% strain, (b) Stress at 30% strain and, (c) Young's modulus

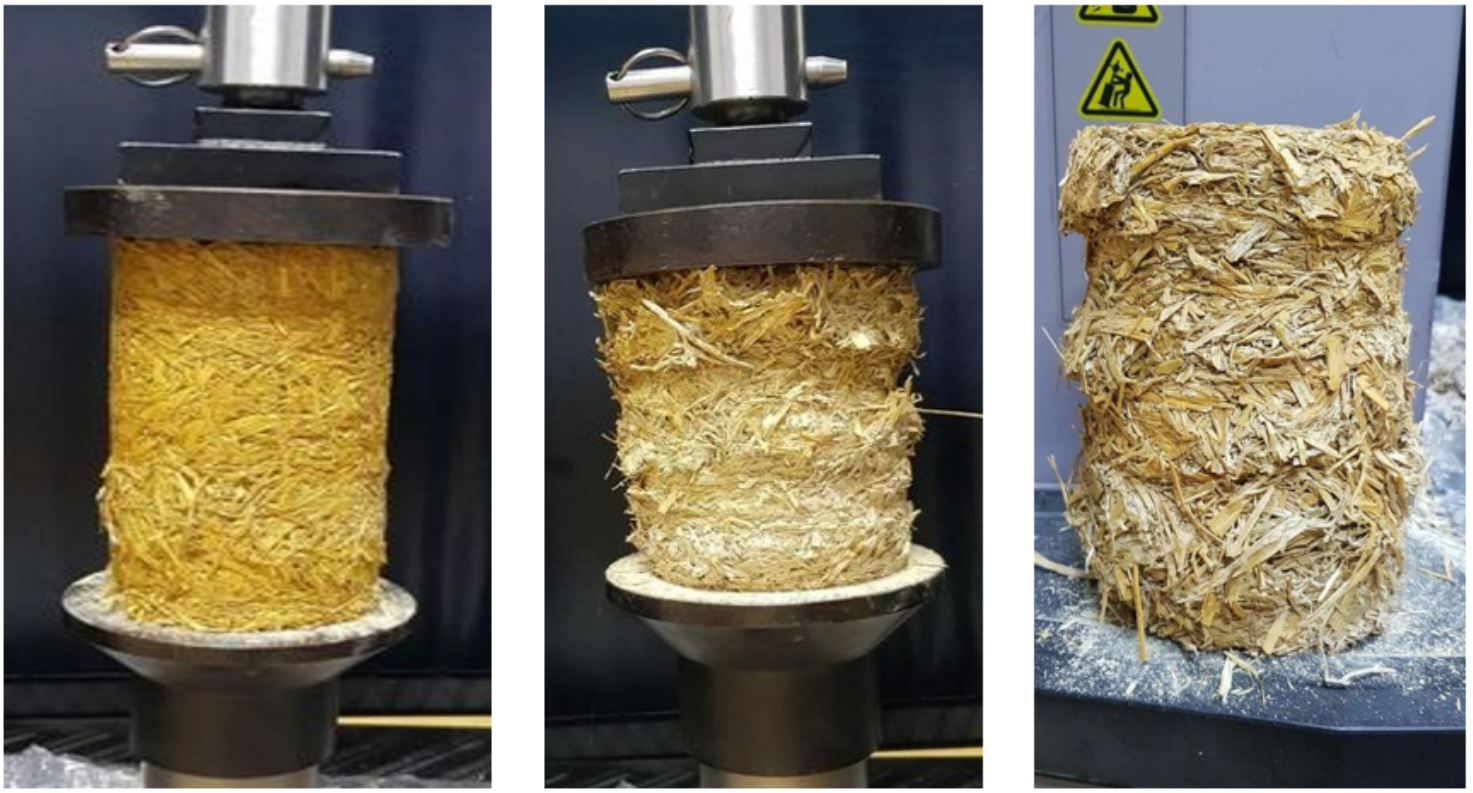

Figure 9

Illustration the specimens under compression tests: (a) before, (b) during and (c) after compression test.

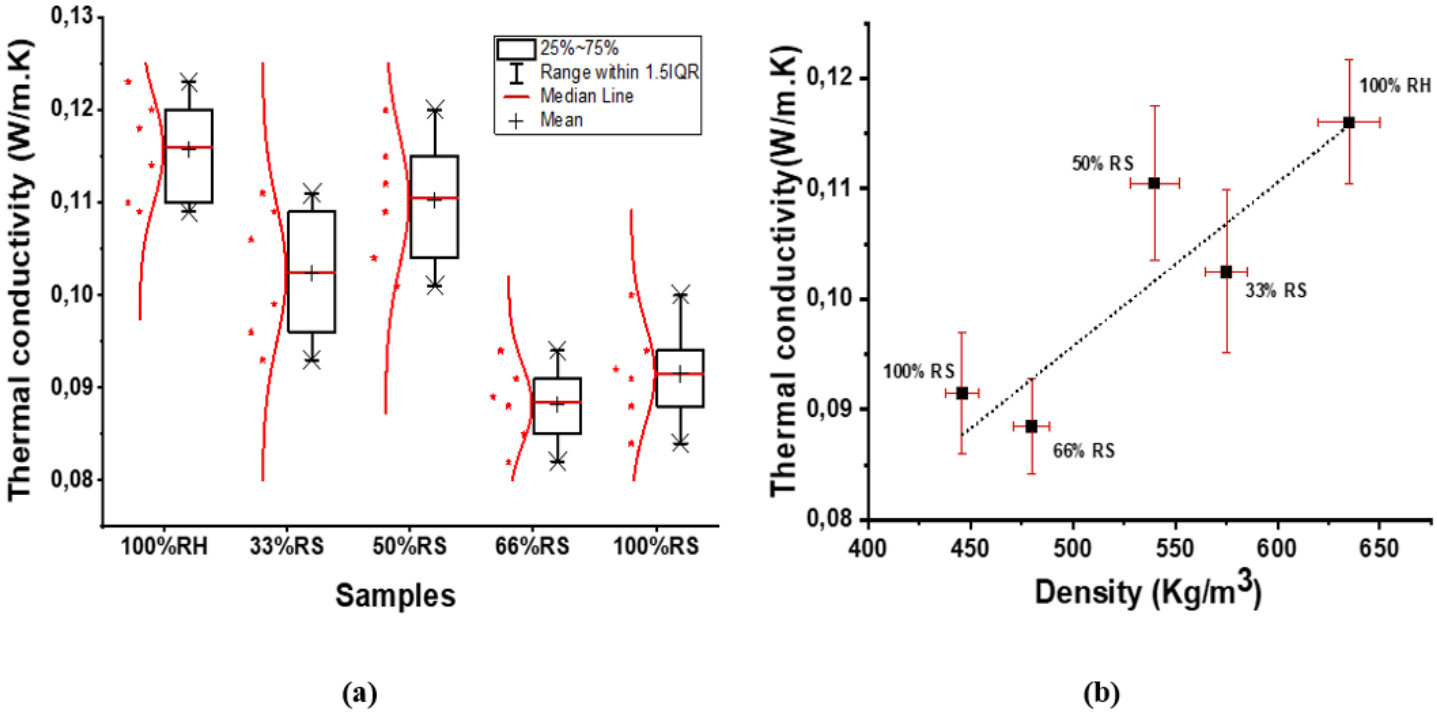

Figure 10

(a) Thermal conductivity of husk/straw- concretes, (b) Thermal conductivity versus density

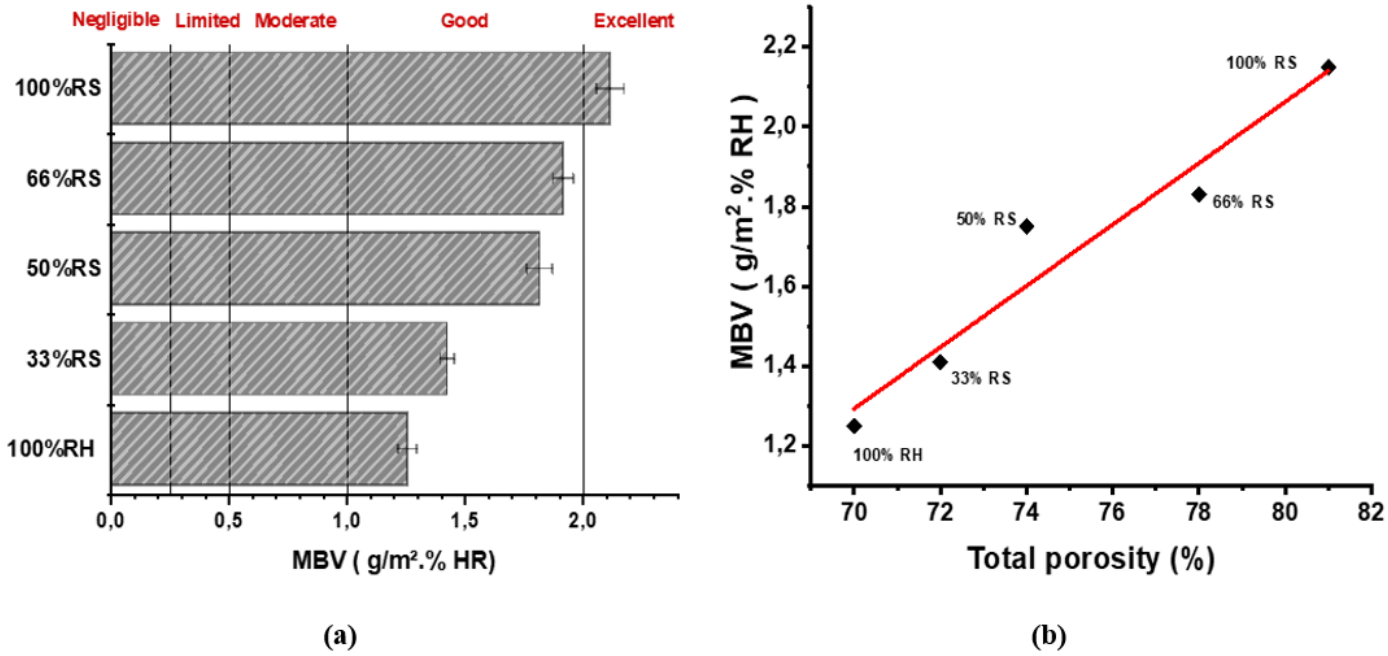

Figure 11

(a) MBV of husk/straw concretes, (b) Moisture buffer value versus total porosity

Supplementary Files

This is a list of supplementary files associated with this preprint. Click to download.

- ga.png